https://doi.org/10.5194/egusphere-2024-3466
Preprint. Discussion started: 7 November 2024

Earth observation for Shrub Encroachment

Irini Soubry[1], Xulin Guo[1]

[1]Geography and Planning, University of Saskatchewan, Saskatoon, S7N 5C8, Canada

Correspondence to: Irini Soubry (irini.soubry@usask.ca)

Abstract. Woody plant encroachment (WPE refers to the increase in density, cover, and biomass of trees and shrubs, affecting both the environment and economy. Many regions lack quantification of WPE, and its driving factors remain unclear. Shrub encroachment, involving woody plants up to 1.5 meters tall, is particularly challenging to quantify due to the lower height and coverage of shrubs. Remote sensing can address this by leveraging spectral and structural properties to improve shrub detection. Integrating accurate quantifications of shrub encroachment over time in models with a variety of potential driving factors can shed light on primary encroachment patterns and mechanisms, aiding local management efforts. We present a case study in the Cypress Upland ecoregion of Canada, where we examine the relationship between 22 different topo-edaphic, anthropogenic, and climatic factors, and shrub cover changes from 2011 to 2018.

1 Summary

Grasslands are rapidly disappearing and degrading worldwide (Bardgett et al., 2021). The spread of unwanted herbaceous and woody plants poses a significant threat to natural grasslands globally. Woody plant encroachment (WPE) involves the increase in density, cover, and biomass of trees and shrubs, whether native or non-native, beyond their historical or geographical ranges (S. R. Archer et al., 2017; Van Auken, 2000). WPE impacts the environment, food industry, and economy. During WPE, grassland insects and animals experience habitat shrinkage; which impacts pollination, breeding areas (Gray & Bond, 2013), and food resources, due to the decline in herbaceous biomass. This, in turn, affects higher food chains, such as carnivores in grasslands (Briske editor, 2017, Chapter 2). Additionally, WPE areas are estimated to support only about 25% of the cattle capacity compared to open grasslands, drastically reducing forage availability (Moss et al., 2008). Over the past 30 years, the U.S. Great Plains lost production value between $4.1-5.6 billion due to WPE (Morford et al., 2022). While grassland conversion to crops is evident, WPE is subtle, and challenging to reverse even with timely management. Despite the risks to ranchers, it is not clear how much grassland is impacted by WPE. Shrub encroachment, involving small woody plants up to 1.5 meters tall, is particularly difficult to quantify due to lower height and coverage.

Remote sensing (RS) data offer several advantages for monitoring shrub encroachment, including large-scale coverage, near-real-time monitoring, cost-efficiency and consistency. Remote sensing data can assist in delineating management priority areas, identifying stages of encroachment, and assessing grassland conditions (e.g., good, fair, poor). Optical RS can detect

https://doi.org/10.5194/egusphere-2024-3466
Preprint. Discussion started: 7 November 2024

shrubs with distinct spectral signatures from surrounding land cover types (Soubry & Guo, 2021). These signatures are influenced by the phenological, biochemical, and structural properties of encroaching shrubs (Skowronek et al., 2017). Depending on the season, vegetation indices related to increasing dry-matter non-photosynthetic materials (e.g. twigs, branches, and dry leaves) perform higher during senescence (e.g., CARI, NDLI, NDNI), while vegetation indices related to higher greenness (i.e. DGVI) perform better during active woody plant growth (Oldeland et al., 2010). Therefore, cloud-free images are crucial when considering phenological stages for shrub mapping. However, when spectral differences between shrub and their background are subtle, there may not be enough variance, leading to mixed classifications and inaccurate results (Royimani et al., 2019). This issue also arises with coarse spatial resolution imagery (Soubry & Guo, 2022).

Nonetheless, shrubs with distinct morphologies and structures might be detectable using object-based image classification approaches (Soubry et al., 2022). Additionally, height information from digital elevation models or LiDAR datasets can enhance shrub detection (Zlinszky et al., 2014), as can multi-angular RS data (Millan & Sanchez-Azofeifa, 2018). Incorporating textural measures from radar data could also improve shrub detection. However, recent studies show that Sentinel-1 SAR data might not yield optimal results for vegetation detection due to its low frequency, which cannot penetrate thick vegetation layers, resulting in backscatter of decreased biomass (Rajah et al., 2019; Smith & Buckley, 2011). The large incident angle of Sentinel-1 might also hinder the detection of vegetation physiology (Ghulam et al., 2011). The upcoming NISAR satellite mission, equipped with L-band and S-band SAR, could offer a solution. Overall, combining spectral, textural, and structural properties, that align with the target plant properties, improves shrub detection (Kopeć et al., 2019).

One of the most pertinent issues in RS quantification of shrub encroachment is early detection. Most multispectral satellite sensors have medium spatial resolution, and are therefore unable to detect early encroachment stages (Lass et al., 2005; Royimani et al., 2019), unless the phenomenon is the same size as the pixel (i.e. for homogeneous and large spread encroachment) (Royimani et al., 2019). The type of RS data used also influences its appropriateness for shrub detection apart from spatial resolution. For instance, in the case of homogenous shrub stands, lower spatial resolution multispectral data may be sufficient, whereas both high spectral and spatial resolution are recommended for species with limited representation in the study area (He et al., 2011). Overall, higher resolution allows for the identification of earlier shrub encroachment stages than does coarser resolution.

2 Anthropogenic, topo-edaphic and climatic drivers of shrub cover change

Shrub encroachment is a global issue, but the factors driving it on grasslands are not fully understood. There is ongoing debate, from which a multitude of local and global drivers has emerged (e.g., climate change, fire regime changes, soil and topography differences, etc.). Global drivers are connected to changes in the Earth atmosphere together with changes in the land use of grasslands, since these happen at a very large scale (Wilsey, 2018, Chapter 7). Environmental drivers are divided

https://doi.org/10.5194/egusphere-2024-3466
Preprint. Discussion started: 7 November 2024

into climatic (regional) and topo-edaphic (local) categories. Climatic drivers include air temperature increases, changes in rainfall intensity, and CO_2 levels (Bond & Midgley, 2012), while topo-edaphic factors involve hydrology, soil, and topography (S. R. Archer et al., 2017). Anthropogenic drivers relate to land use and vegetation management changes. These changes can be related to land conversions to agriculture, and growth of population centers, leading to infrastructure (e.g., power lines, roads, fences), which provide for woody propagules. Worldwide, between 1992 and 2015 alone, 25% of all land conversions came from grasslands (Strassburg et al., 2020).

2.1 Climatic

Global warming may lead to declines in grass cover due to drought, allowing woody species to thrive by accessing moisture with their deeper roots (Polley et al., 2013). Research indicates that WPE is promoted by increased precipitation intensity up to a certain limit (Scholtz, Fuhlendorf, et al., 2018). A review of 29 studies across 13 different grassland and savanna areas found that plant species declined by an average of 45% following woody encroachment, with areas of high precipitation being more affected (Wilsey, 2018, Chapter 8). Additionally, CO_2 concentrations have risen from about 270 ppm in the mid-1800s to approximately 400 ppm in 2017, and are projected to reach 550 to 700 by the end of the 21st century (Wilsey, 2018, Chapter 7). Previous studies have yielded mixed results when attempting to link increased CO_2 levels with WPE. Global vegetation models suggest that higher CO_2 levels strengthen woody plants (Bond & Midgley, 2012). Specifically, the rise in CO_2 facilitates photosynthesis for C_3 species (e.g. small shrubs) more than for C_4 species (e.g. warm-season grasses) (Polley et al., 2013). However, Archer et al. (2017) found WPE often progresses faster than CO_2 increases, indicating that while CO_2 may play a role, it is not the primary driver of WPE. Körner et al. (2006) suggest that the change in woody plant cover should be significant enough to compare with CO_2 enrichment values necessary for substantial growth changes, which is a difference of more than 160 ppm over the years.

2.2 Topo-edaphic

Hydrology, topography, and soil properties are local factors that influence the development of woody plants in grasslands. Grasslands and woodlands differ structurally in these aspects. Woody plants, with their larger and deeper roots, thrive in deeper soils and can reduce competition with grasses for soil moisture. While grasslands remain dormant for part of the year, and transpiration and rainwater interception occur over a shorter timeframe. Specific soil properties, such as texture and depth, can prevent shrub encroachment (Briske editor, 2017, Chapter 2). For instance, shallow and dry soils can limit woody plant encroachment (Bragg & Hulbert, 1976; Pracilio et al., 2006). Drought generally reduces woody cover in grasslands and savannas, particularly affecting species with low growth rates before drought or those dependent on deeper soil moisture. Shrub encroachment can also impact hydrological cycles in areas with shallow aquifers, as woody plants can trap more moisture in the air, leading to increased cloud formation and rainfall (S. Archer et al., 2001). Lastly, variations in woody plant distribution based on topography can be explained by differences in solar radiation, precipitation, and slope aspects (Kennedy, 1976).

https://doi.org/10.5194/egusphere-2024-3466
Preprint. Discussion started: 7 November 2024

2.3 Anthropogenic

Anthropogenic drivers of shrub encroachment, such as land abandonment and protection, land fragmentation, changes in grazing regimes, and alterations in fire frequency, intensity, and cover, play a significant role in transforming grassland ecosystems. In mountainous grassland areas, the highest encroachment rates were observed in regions with significant land abandonment (Gartzia et al., 2014). Similar trends were noted in ungrazed grasslands (Bogunovic et al., 2019), and in the desert grasslands of southeastern Arizona, which were protected for a 74-year period (Browning et al., 2014). Specifically, high-density shrub patches increased over time by forming clusters at small distances, which eventually filled in. The fragmentation in grasslands due to human infrastructure, such as tree plantations, cities, or homesteads, further increases woody propagule pressure (Briggs et al., 2005). Overgrazing is a major cause of grassland degradation due to higher forage demands, leading to the clearing of grass biomass, reduced grass recovery, and the dispersal of shrub seeds through livestock movement (Eldridge et al., 2013; Kwon et al., 2016; Wang et al., 2019). Nevertheless, the relationship between grazing and WPE remains debated, as a meta-analysis found no consistent link between grazing and shrub cover changes (Briske editor, 2017, Chapter 2). Remote sensing studies suggest a connection, but ground-based studies do not, possibly due to lower spatio-temporal resolution (Ma et al., 2019).

Changes in fire frequency, intensity, and cover are key drivers of shrub encroachment (Bailey et al., 2010; Twidwell et al., 2013). Historically, woody plants were confined to areas with infrequent fires, but it is argued that overgrazing has reduced fine fuels necessary for natural grassland fires (Kwon et al., 2016). Without fire, woody plants grow taller and become fire-resistant, making subsequent fires less effective (Bond & Midgley, 2000). Studies show that areas not treated by fire or herbicide saw significant increases in woody plant encroachment (Bragg & Hulbert, 1976; Scholtz, Polo, et al., 2018). Public policies often limit the use of prescribed fires, reducing their effectiveness (Twidwell et al., 2013). While burning can reduce woody plant establishment, it can also create conditions for woody seedlings to thrive (Mazía et al., 2019). Combining prescribed fires with moderate to heavy grazing has been suggested to conserve species diversity and promote native plants (Beck et al., 2015; Briske editor, 2017, Chapter 2; Hendrickson et al., 2019; O'Connor, 2019; Twidwell et al., 2013; Wang et al., 2019). Thus, the effects of fire and grazing on shrub encroachment depend on the context and remain an open question. Overall, the potential driving mechanisms of shrub encroachment belong to a complex web of local and global factors. As of today, the debate regarding these drivers is still ongoing.

3 Case study in Cypress Upland

Despite the potential of RS to address many ecological limitations in WPE studies, its usage has been limited. This is particularly unexpected given that WPE occurs over large areas with specific spatial patterns and over extended timespans (Buenemann, 2007). Our research over the past five years reviewed 405 WPE-related studies, revealing that 67% focused on WPE ecology, 24% utilized remote sensing, and less than 10% involved modeling. Similarly, a systematic review in 2007 found that only 4.9% of WPE studies were published in geographical journals (Buenemann, 2007). This underrepresentation

https://doi.org/10.5194/egusphere-2024-3466
Preprint. Discussion started: 7 November 2024

of RS and modeling studies partially explains the lack of comprehensive landscape to global-level understandings of WPE cover and processes. To achieve a broader and global understanding of WPE, more transnational, multi-departmental collaborations are needed.

Even though there are challenges in understanding the ecology and applying RS approaches for quantifying WPE, integrating these fields with modeling could help address gaps in the literature (Soubry & Guo, 2022). Effective management of WPE requires considering both local and global driving factors (Stevens et al., 2017). Models can identify these factors by using predictor variables to determine which contribute more to woody plant presence on the landscape. Since WPE is dynamic and progresses over time, time series mapping can reveal long-term patterns and trends, as well as their connections to local and global drivers (Gavier-Pizarro et al., 2012). For instance continuous changes in woody cover from 1986 to 2016 have been correlated with temperature and rainfall patterns to understand the climatic factors driving WPE (Venter et al., 2018). Image change detection analysis is particularly useful for quantifying shrub overlap (stable cover), shrub expansion and reduction. Examples of change detection methods include post-classification change detection, change classification, band difference, band ratio, Euclidean distance, and change vectors (Jensen, 2008; Parelius, 2023).

We use Cypress Hills Interprovincial Park (CHIPP) (49° 40’ N, 110° 15’ W) (**Fig. 1**) as a case study area, where shrub cover using an object-based image classification approach (overall accuracy >92%) was estimated from an aerial image obtained in 2018 (see Soubry et al. (2022)). We obtained an additional set of RGB aerial imagery for 2011 (27 June & 3 July, 40cm spatial resolution) from the Ministry of Parks, Culture and Sports through the FlySask program (https://www.flysask2.ca/) to obtain shrub cover for 2011. Then we conducted change detection analysis to connect changes in shrub cover with potential drivers. A total of 22 topo-edaphic, anthropogenic, and climatic variables were selected for analysis and modelling against shrub cover changes in the park between 2011 and 2018 (**Table 1**).

https://doi.org/10.5194/egusphere-2024-3466
Preprint. Discussion started: 7 November 2024

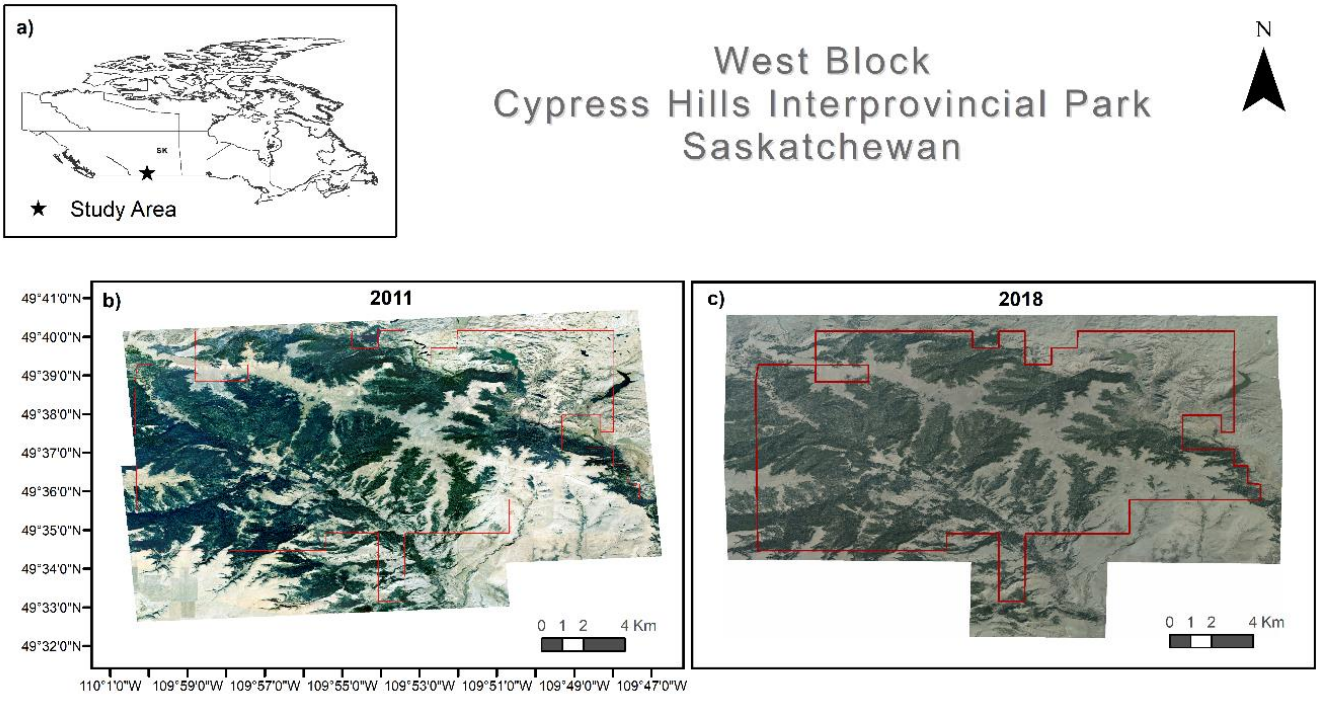

Figure 1: a) West Block of Cypress Hills Interprovincial Park (CHIPP) in Saskatchewan (SK), Canada, b) West Block of CHIPP overlaid on the 8-bit mosaicked 40 cm aerial image of June 27th and July 3rd 2011, c) West Block of CHIPP overlaid on the 8-bit mosaicked 30 cm aerial image of 17 October 2018. Sources: Canadian Provincial Boundaries - Statistics Canada (Open-Government License—Canada) (Statistics Canada, 2020), Aerial image & CHIPP boundary layer: Ministry of Parks, Culture, and Sports, Government of SK.

Table 1 Topo-edaphic, anthropogenic and climatic data layers (for topo-edaphic variables see Soubry et al. (2022), for anthropogenic variables see Soubry et al. (2024))

Category	Variable	Details	Data type	Source
Topo-edaphic (fixed)	Landscape Unit	Combination of Rangeland Ecosite & Topography class	Categorical	2018 CHIPP Forest Inventory
	Rangeland Ecosite	Defined from topography, soil texture, moisture regime, salinity	Categorical	
	Elevation	Upland & Lowland (above and below average elevation)	Categorical	Saskatchewan Geospatial Imagery Collaborative (SGIC)
		15 m resolution	Continuous	
	Aspect	4 compass directions	Categorical	Derived from SGIC Digital Elevation Model (DEM)
	Slope	Classes of 10% slope rise	Categorical	
			Continuous	
	Topography	Depressional, Flat, Gully, Hilly, Steep,	Categorical	2018 CHIPP Forest

https://doi.org/10.5194/egusphere-2024-3466
Preprint. Discussion started: 7 November 2024

Category	Variable	Details	Data type	Source
		and Undulating		Inventory
	Soil Moisture Regime (SMR)	Based on moisture availability for vegetation	Categorical	
	Distance from watercourse lines	Euclidean distance, 15 m spatial resolution (Part of the "Lakes, Rivers and Glaciers in Canada-CanVec Series-Hydrographic Features")	Continuous	Government of Canada
	Distance from wetlands	Euclidean distance, 15 m spatial resolution (Digitized by Geomatics Canada)	Continuous	National Topographic Data Base
	Distance from waterbodies	Euclidean distance (15 m spatial resolution)	Continuous	Ministry of Parks, Culture and Sport (Saskatchewan, Canada)
Anthropogenic	Grazing	Park Managers' perception on grazing intensity (Low, Low-Medium, Medium, Medium-High, High)	Categorical	Spatial layer by Ms. Larissa Robinov from interview with Mrs. Melody Nagel-Hisey and Mr. Kevin Redden (Park Managers)
	Distance from roads	Total road network	Continuous	Ministry of Parks, Culture & Sports – reviewed by Mrs. Melody Nagel-Hisey
	Haying impact	Haying frequency	Categorical	
		Years since last hay	Continuous	
		Hayed vs. Non hayed areas	Categorical	
Climatic	Daily Total Precipitation	Sum of all forms converted to water-equivalent ("prcp")	Continuous	DayMet v4.4 (Thornton et al., 2022)
	Min & Max daily Temperature	Daily 2-m air temperature ("tmin", "tmax")	Continuous	
	Annual Heat Moisture Index	Combined effects between precipitation and evaporation/transpiration	Continuous	(Hewins et al., 2018)
Spectral	Normalized	Atmospherically corrected surface	Continuous	Landsat 5,7,8,9

https://doi.org/10.5194/egusphere-2024-3466
Preprint. Discussion started: 7 November 2024

Category	Variable	Details	Data type	Source
	Difference Vegetation Index	reflectance between 1990 and 2022		
	Shrub cover	Shrub presence in 2018 at 30 cm spatial resolution	Continuous	Soubry et al. (2022) and Ministry of Parks, Culture & Sports

3.1 Methods

3.1.1 Image classification

We applied the same processing steps as in Soubry et al. (2022) to derive shrub cover for the grassland areas of CHIPP in 2011. We calculated statistical, geometrical, spectral, and textural attributes (**Table 3**), and we collected 1200 training objects and 800 validation objects for each class (i.e., 'Shrub' and 'No Shrub').

Table 2 Attributes used for 2011 shrub cover classification using an object-based SVM method (SVM: Support Vector Machine, R: Red, G: Green, B: Blue, GRVI: Green/Red Vegetation Index, GI: Greenness Index)

Attribute Category	Attributes	Channels Used
Statistical	Min, Max, Mean, Standard Deviation	R, G, B
Geometrical	Circularity, Compactness, Solidity	/
Spectral	GRVI, GI*	R, G
Textural**	Mean, Standard Deviation, Entropy, Angular second moment	R, G, B

* All other indices required the presence of a NIR band

**For a 5x5 pixel window

During post-classification editing we dissolved the shapes for each "shrub" and "no shrub" object and calculated the average shrub cover over the total grassland area in the park (i.e., 49.6%). Our estimate was very high and potentially over-estimating shrub cover. Therefore, we applied a rule-based classification. From the shrub class, we removed the objects that had negative values and low values up to 0.04 for the GRVI index. Negative values correspond to bare ground and soil. Moreover, values between 0 and 0.04 are most likely grasses. This decision was based on three separate observations of datasets:

i) GRVI ((Green - Red) ÷ (Green + Red)) for summer reflectance of shrub and grass cover obtained with a field spectroradiometer in 2020 in Kernen Prairie, SK, Canada (Soubry & Guo (2021)). We used the mean simulated

https://doi.org/10.5194/egusphere-2024-3466
Preprint. Discussion started: 7 November 2024

reflectance value (%) from the Green and Red bands of Landsat-8 and Sentinel-2A of 0% shrub cover in the summer. That gave us a GRVI-Landsat-8=0.05 and a GRVI-Sentinel-2A=0.07.

ii) GRVI for field obtained endmembers of shrubby cinquefoil (one of the dominant shrubs in of CHIPP West Block) and quadrat spectra of different shrub cover percentages in the West Block of CHIPP from the summer of 2021. We used the mean simulated reflectance value (%) from the Green and Red bands of Landsat-8 and Sentinel-2A. For 0% shrub cover GRVI-Landsat-8=0.03, and GRVI-Sentinel-2A=0.05.
iii) based on the attribute visualization in PCI Geomatics.

We considered that the spectral data from CHIPP West Block quadrats is more appropriate as it corresponds to the same study area. Therefore, we selected a GRVI threshold value between 0.03 and 0.05, which is 0.04. In the end, the average shrub cover in 2011 was re-calculated.

Lastly, the annual rate of shrub cover change between 2011 and 2018 was calculated using equations:

$$q = \left(\left(\frac{A2}{A1}\right)^{\frac{1}{(t2-t1)}} - 1\right) x\ 100 \qquad \text{(FAO (1995))} \ \textbf{(1)}$$

$$\frac{1}{t2-t1} \ln\left(\frac{A2}{A1}\right) x\ 100 \qquad \text{(Puyravaud (2003))} \quad \textbf{(2)}$$

Where,

- t2-t1 is the total time of the change detection
- A2 is the total shrub cover in time t2, A1 is the total shrub cover in time t1.

3.1.2 Change detection analysis

The 2018 shrub cover classification (30 cm) was resampled to the spatial resolution of the 2011 classified image (40 cm). Both images were georegistered to eliminate spatial error during change detection (PCI Geomatics Banff 2018 Focus). Image differencing was used for change detection (ArcMap version 10.8.2). Percent cover for each shrub cover class (stable, expansion, reduction) over the total grassland area in the park was calculated. The shrub reduction layer was excluded in the driving factor analysis due to lower confidence.

3.1.3 Driving factor analysis

Topo-edaphic, anthropogenic and climate factors that contribute to expansion of shrub cover, and conditions that contribute to stable cover between years are explored. Growing season trends and long-term climate trends of the study area are also analyzed. The layers of shrub expansion and stable shrub cover were compared with each variable of **Table 1** to determine

https://doi.org/10.5194/egusphere-2024-3466
Preprint. Discussion started: 7 November 2024

the percent change in shrub cover (similar to the approach in Soubry et al. (2024). The topo-edaphic variables remained constant between the two years. However, changes between 2011 and 2018 were considered for the anthropogenic variables.

Climate data analysis

Most time-series that use climate data to compare with WPE require continuous woody cover (e.g., Venter et al. (2018)). However, Skowno et al. (2017) examined changes in woody cover between 1990 and 2013 to create a change map, which they compared with binned mean annual precipitation. Given that we have two dates for shrub cover, we adopted Skowno et al.'s (2017) approach. Between the CHIRPS, WordClim, ERA5, and DayMet v4.4 datasets, we selected the DayMet dataset due to its spatial resolution (1x1 km), its availability in North America, the long-term available timespan for the study area (1981-2022), the fact that data is extrapolated and interpolated from weather stations, and because of daily temperature and precipitation variables. DayMet data for our study stems from two nearby weather stations located in the East Block of the park.

All DayMet data was processed in Google Earth Engine (GEE). Mean daily temperatures were calculated by adding "tmin" and "tmax" and dividing by two. Total annual precipitation, mean annual temperature and their standard deviations were calculated for each year from 2011 to 2018 for each 1x1 km pixel using their daily values inside the CHIPP park boundaries. Then, the mean values across years for each pixel were calculated. The total mean annual precipitation (MAP) and mean annual temperature (MAT) were exported from GEE and used to generate gridded precipitation and temperature maps. The average of three rules defined the number of bins for the precipitation data:

i) The square root rule: Number of Bins= sqrt(Number of Data Points)=sqrt(266)=**16**
ii) Sturges' rule: Number of Bins=1+$\log_2$(Number of Data Points)=1+$\log_2$(266)=3.42=**3** (Sturges, 1926)
iii) Rice Rule: Number of Bins=2×(Number of Data Points)$^{1/3}$=2x(266)$^{1/3}$=**12** (Lane, 2008)

The average was 10 bins, with a 9 mm range for each if we assume equal interval, similarly to Skowno et al. (2017). For better interpretation, we used 9 bins of 10 mm. We used the same approach for temperature data, resulting in 8 bins of 0.15 degrees Celsius.

Strong altitudinal differences in the park highly affect temperature and plant moisture requirements. To understand the combined effects between precipitation and evaporation/transpiration (which is a function of temperature) on shrub cover, we calculated the gridded Annual Heat Moisture Index (AHM) = (MAT + 10) / (MAP/1000) and their standard deviations as described in Hewins et al. (2018). Lower values represent colder and wetter climate, while higher values warmer and drier climate. Gridded AHM data was separated into 7 bins of 1 AHM unit. To find the tipping point for net shrub cover increase depending on the AHM value, we used continuous data.

We further examined long-term climate trends from 1981 to 2022 to better understand the climate effects in the study area. We calculated the MAP, MAT, and AHM for each year within this period and plotted trendlines. To test for statistical

https://doi.org/10.5194/egusphere-2024-3466
Preprint. Discussion started: 7 November 2024

significance, we used the Mann-Kendall test. Seasonality was not removed since annual data averages out seasonal fluctuations. Lastly, we did not include CO_2 concentrations in our analysis because the increase of 100 ppm between 1860 and 2013 in Canada found by Cheng et al. (2022) is below the 160 ppm threshold needed to induce woody plant growth, as per Körner et al. (2006).

Growing season analysis

To assess the impact of climate change on the grassland ecosystem within CHIPP, we calculated Normalized Difference Vegetation Index (NDVI) time series using atmospherically corrected surface reflectance from Landsat 5, 7, 8, and 9 images between 1990 and 2023. Through GEE processing, we selected images with <30% cloud cover and applied a cloud mask, resulting in 480 images. A 15-day moving average smoothed the NDVI time-series chart. We then analyzed seasonal trends over the years by selecting three months to represent the start, peak, and end of the growing season. May, having the lowest NDVI value for most years, was chosen as start of season. July, with the highest NDVI value, was selected as peak, and September, showing declining NDVI values between 0.15 and 0.05 for most years from 1990 to 2023, was chosen as end of season. Then, the monthly averages of all available NDVI values for each month were plotted as seasonal time-series. Finally, the annual average NDVI was computed to compare with trends in MAP, MAT, and AHM.

Modeling

To analyze the combined relationship between all variables in **Table 1** and annual percent shrub cover change in the park, multiple models were developed (**Table 3**). Climatic variables were excluded due to their coarser resolution (1x1 km). The dependent variable in each model is net shrub cover change between 2011 and 2018 for each 15x15m grid cell. This spatial resolution was chosen because of the available DEM. First total percent change between 2011 and 2018 (ranging from -100 to +100) was calculated, then annual percent change. Due to varying data coverage and missing values, independent variables for nine models were selected based on spatial co-occurrence, resulting in different sample sizes. We used a generalized least squares (GLS) regression and checked for multicollinearity among continuous variables, finding no significant correlations. Variables were standardized before running the models to rank the model coefficients by importance. Scripts were developed in RStudio (RStudio Team, 2021) using the "nlme" package with the gls() function (Jose Pinheiro et al., 2013). After running the models, we accounted for spatial autocorrelation in the residuals as in Soubry et al. (2024). Due to high hardware requirements, model processing was transferred to the High-Performance Computing (HPC) cluster at the University of Saskatchewan. For some models (1a, 1b, 1c, 1d, 3b1, and 3b2), the sample size was reduced to a random subset to ensure timely processing.

https://doi.org/10.5194/egusphere-2024-3466
Preprint. Discussion started: 7 November 2024

260 **Table 3 Models used to examine the combined relationship between topo-edaphic and anthropogenic variables and shrub cover changes between 2011 and 2018 in the park**

Model	Type	Independent variables	Selected spatial structure accounting for RSA	Sample size
1a	Topo-edaphic	Elevation, Slope Rise, Topography, Range Ecosite, Aspect, Landscape Unit, Soil Moisture Regime, Distance from watercourse lines, Distance from waterbodies	Rational Quadratic	100,000
1b		Elevation Categorical, Slope Rise Categorical, Topography, Range Ecosite, Aspect, Landscape Unit, Soil Moisture Regime, Distance from watercourse lines, Distance from waterbodies	Rational Quadratic	100,000
1c		Elevation, Slope Rise, Topography, Range Ecosite, Aspect, Landscape Unit, Soil Moisture Regime, Distance from watercourse lines, Distance from waterbodies, Distance from wetlands	Rational Quadratic	40,000
1d		Elevation Categorical, Slope Rise Categorical, Topography, Range Ecosite, Aspect, Landscape Unit, Soil Moisture Regime, Distance from watercourse lines, Distance from waterbodies, Distance from wetlands	Rational Quadratic	40,000
2a	Anthropogenic	Road Distance, Grazing Intensity, Haying Frequency, Years Since Last Hay,	Exponential	7,566
3a1	Mixed	Elevation, Slope Rise, Road Distance, Topography, Range Ecosite, Aspect, Grazing Intensity, Landscape Unit, Haying Frequency, Years Since Last Hay, Distance from watercourse lines, Distance from waterbodies	Rational Quadratic	7,158
3a2		Elevation, Slope Rise, Road Distance, Range Ecosite, Aspect, Landscape Unit, Haying Frequency, Years Since Last Hay, Distance from watercourse lines, Distance from waterbodies, Distance from wetlands	Exponential	888
3b1		Elevation, Slope Rise, Road Distance, Topography, Range Ecosite, Aspect, Grazing Intensity, Landscape Unit, Hayed,	Rational Quadratic	30,000

https://doi.org/10.5194/egusphere-2024-3466
Preprint. Discussion started: 7 November 2024

Model	Type	Independent variables	Selected spatial structure accounting for RSA	Sample size
		Soil Moisture Regime, Distance from watercourse lines, Distance from waterbodies		
3b2		Elevation, Slope Rise, Road Distance, Topography, Range Ecosite, Aspect, Landscape Unit, Hayed, Soil Moisture Regime, Distance from watercourse lines, Distance from waterbodies, Distance from wetlands	Rational Quadratic	10,000

3.2 Results

3.2.1 Image Classification and Change detection

The classification of the 2011 orthomosaic resulted in an overall accuracy of 91.3% based on visual photointerpretation (95% Confidence Interval between 89.7% and 92.9%). The producer's and user's accuracy for each class were above 88.0%. The average shrub cover in the grassland areas of the West Block in CHIPP was 27.13% for 2011, with a 1.95% increase in shrub cover % between 2011 and 2018. The annual rate of shrub cover change between 2011 and 2018 is 0.995%/year according to **Equation 1**, and 0.990%/year according to **Equation 2**. **Figure 2** shows annual percent shrub cover change in the West Block of CHIPP. Between 2011 and 2018, 10.6% of the shrub cover in the grassland area of the park remained stable, 16.2% expanded, and 16.5% reduced, while 56.7% of the grassland area of the park had no shrub cover.

https://doi.org/10.5194/egusphere-2024-3466
Preprint. Discussion started: 7 November 2024

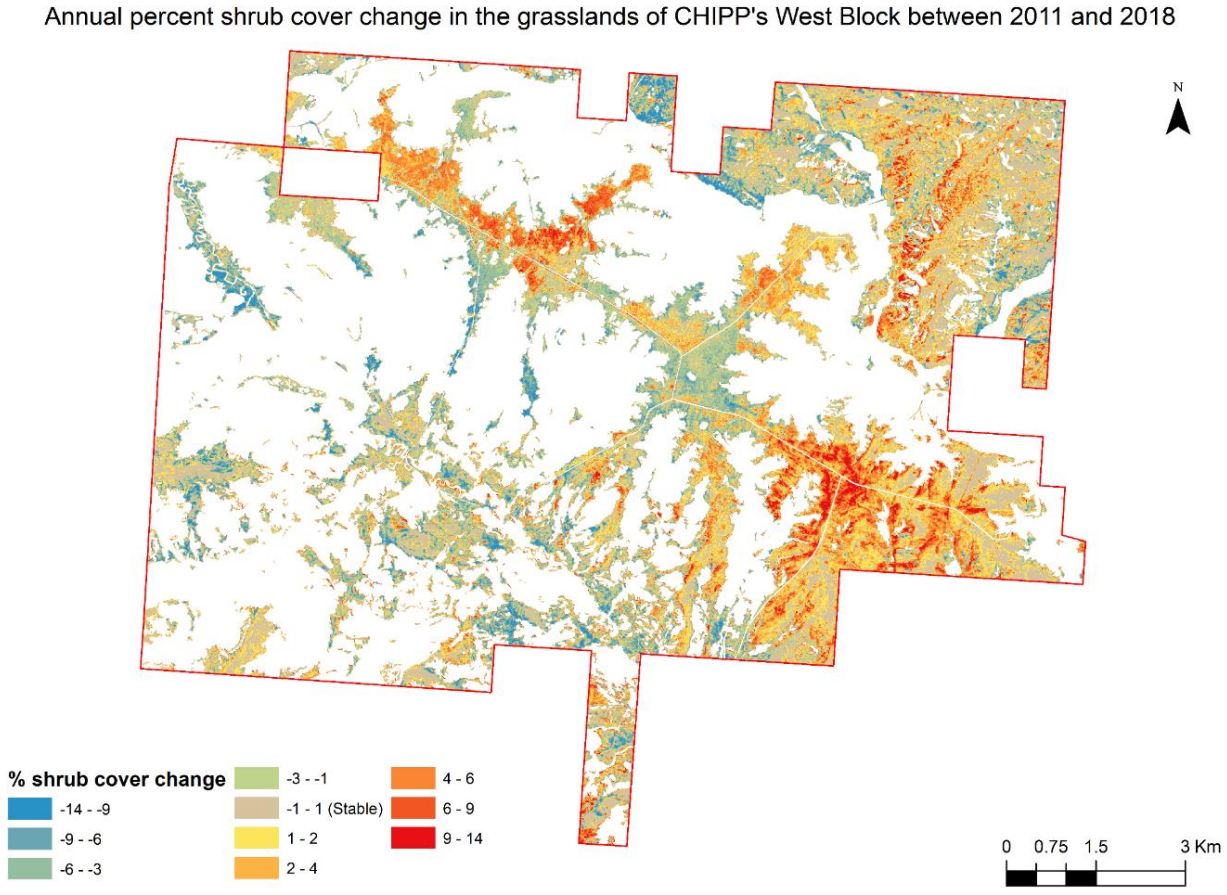

Figure 2 Annual percent shrub cover change in the grasslands of CHIPP's West Block between 2011 and 2018.

3.2.2 Driving factors

Topo-edaphic

Flat areas had the highest total shrub expansion and stable shrub cover relative to their total area (20.4% and 13.0%, respectively). Specifically, 49.1% of total shrub expansion and 48.0% of stable shrub cover occurred on Flat topography, with 38.5% and 36.6% on Loam-Flat landscape units. Loam ecosites accounted for 68.2% of shrub expansion and 63.9% of stable cover.

Steep slopes (220-230% rise) had the highest shrub expansion (27.3%), while shallower slopes (10-20% rise) had the highest stable cover (12.2%) compared to their total area. Most shrub expansion (74.4%) and stable cover (68.2%) occurred on slopes between 0% and 10% rise. Upland grasslands had more shrub expansion (19.0%) compared to lowland grasslands (13.3%), while stable cover was similar (10.4% and 10.8%).

https://doi.org/10.5194/egusphere-2024-3466
Preprint. Discussion started: 7 November 2024

Very Fresh soil moisture regimes (SMR) had the highest shrub expansion and stable cover (19.1% and 20.1%). Moderately Fresh soils saw 69.1% of shrub expansion and 58.9% of stable cover, while Very Moist SMR sites had the lowest (0.02% and 0.04% respectively). This could explain why shrub expansion increased with distance from waterbodies and wetlands (peaking around 2 km from the waterbodies with significant correlations; r^2 = 0.19 and 0.08, p < 0.001). Stable cover decreased with distance from waterbodies. No clear relationship was found between distance from watercourses and shrub expansion.

Anthropogenic

Medium-High grazing intensity areas experienced the most significant shrub expansion relative to their total area (33.3%), whereas Low-Medium grazing intensity areas saw the least (12.3%). High intensity grazing areas maintained the highest stable shrub cover (18.4%), while Low-Medium grazing areas had the lowest (4.4%) relative to their total area. Additionally, Medium grazing intensity areas accounted for 50.1% of the total shrub expansion, followed by High grazing intensity areas (36.3%). Low grazing intensity areas contributed the least to total shrub expansion (2.7%). Moreover, shrub expansion was higher closer to roads (r^2=0.32, p < 0.001). Conversely, stable shrub cover appeared consistent across various distances from the road network.

Overall, in the hayed areas of the park, a lower percent of its area was undergoing any type of change related to shrub cover compared to the non-hayed areas. 12.4% of the hayed areas of the park had shrub expansion, and 2.5% had stable shrub cover, while 16.5% of the non-hayed areas in the park underwent shrub expansion and 11.2% had stable shrub cover between 2011 and 2018. Areas hayed before 2011 experienced the highest shrub expansion, with an increase of 15.7% relative to their total area. In contrast, areas hayed only once or twice between 2011 and 2018 saw slightly lower shrub expansion rates of 9.8% and 10%, respectively. Stable shrub cover exhibited a similar trend but at much lower levels. Notably, areas hayed twice between 2011 and 2018 had the lowest shrub expansion at 3.2%, while the majority of shrub expansion (52.2%) occurred in areas hayed before 2011. Stable shrub cover followed a comparable pattern.

Climatic

Net shrub cover increases are observed in the wettest areas of the park, with precipitation ranging from 536 mm to 556 mm. The second wettest area shows the highest annual shrub cover increase at 0.006%. Shrub cover remains stable in regions with precipitation between 505 mm and 515 mm. Over a 40-year period (1981-2022), there is a slightly positive linear trend in precipitation (p <0.05). The mean annual precipitation (MAP) increased at an average rate of 155 mm/year, with the mean total annual precipitation for this period being 506 mm. Shrub cover increased in the second coldest area of the park (3.2 to 3.3°C) and decreased in all other temperature ranges, suggesting a preference for colder conditions. Over the 40-year period from 1981 to 2022, there is a significant positive linear trend in temperature (p <0.05). During this time, the annual mean temperature increased by an average of 0.97°C per year, with the mean annual temperature being 2.75°C. This trend is further highlighted in the AHM index, which shows the highest shrub expansion in the coldest and wettest areas of the park,

https://doi.org/10.5194/egusphere-2024-3466
Preprint. Discussion started: 7 November 2024

while warmer and drier areas experienced a net decline in shrub cover (**Fig. 3, Fig. 4**). The tipping point for net shrub cover
315 increase occurs at AHM values below 25.5 (95% confidence interval 24.9 - 26.1 AHM units).

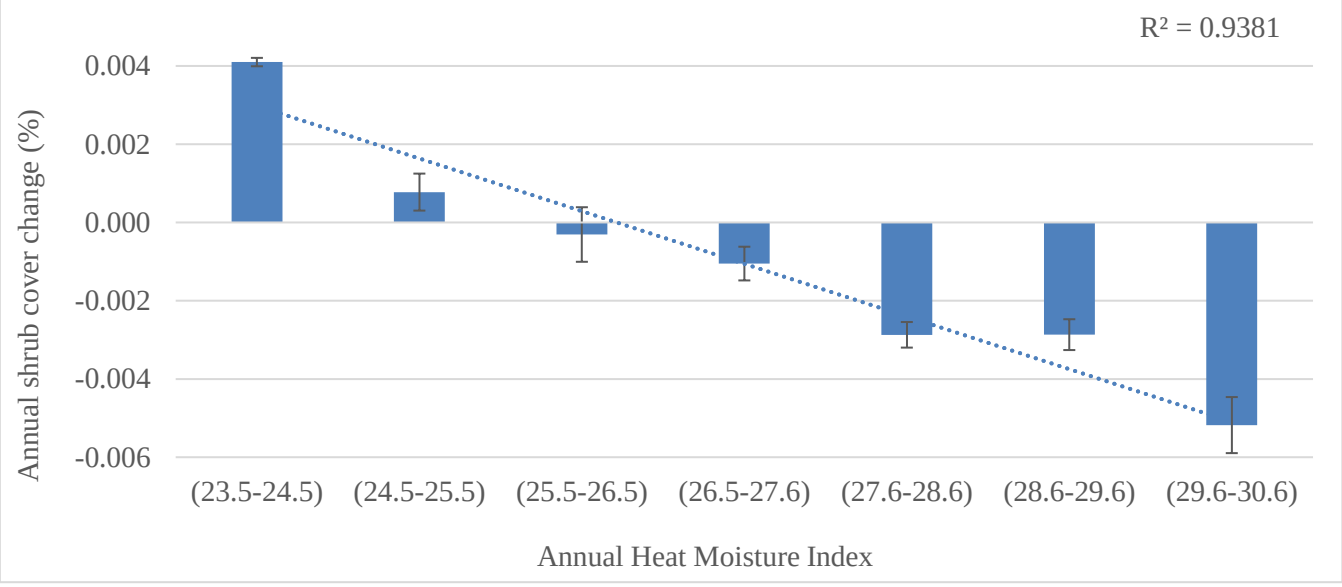

Figure 2 Annual Heat Moisture index bins versus annual shrub cover change percent from 2011 to 2018 in Cypress Hills Interprovincial Park, West Block, Saskatchewan, Canada (the error bars represent standard error with a scaling factor of 0.0005).

https://doi.org/10.5194/egusphere-2024-3466
Preprint. Discussion started: 7 November 2024

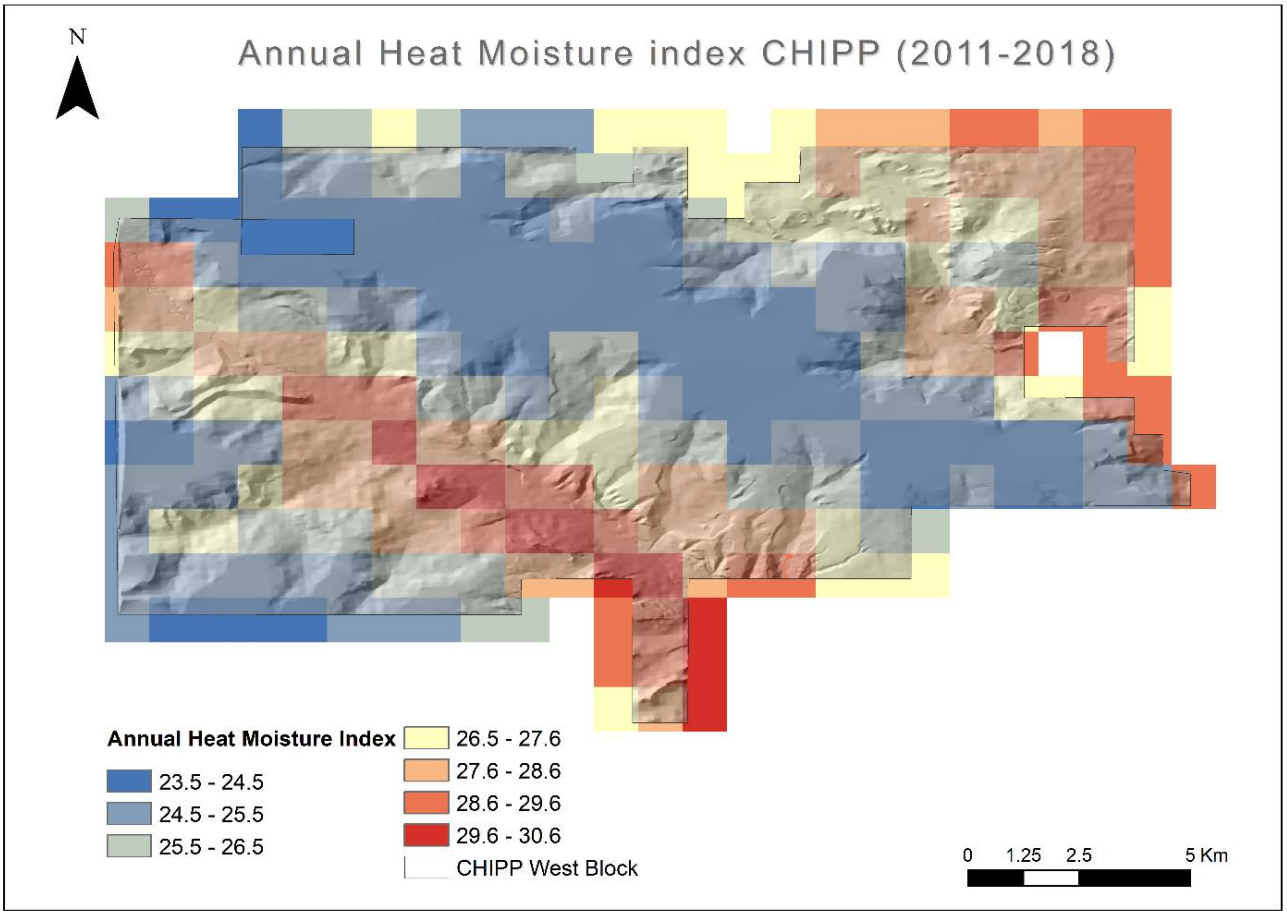

320 **Figure 3 Map of the Mean Annual Heat Moisture Index between 2011 and 2018 in increment bins of 1 in Cypress Hills Interprovincial Park, West Block, Canada.**

Growing season analysis

The 15-day average NDVI time-series (1990-2023) show a relatively stable pattern across years, with high interannual variation (**Fig. 5**). Significant dips in NDVI peak values correspond to very hot and dry years (red arrows) or wet and cold
325 years (blue arrows). The mean annual NDVI time-series exhibits a slight positive trend (r^2=0.05), indicating increased vegetation growth and greenness over time (**Fig. 6**). There is considerable variation across years, with fewer extreme low NDVI values from 2005 and onwards. Confidence in the time-series improves over time as the number of available Landsat images increases. For the peak of the season (July), there is a slight positive trend (r^2=0.07), suggesting more green vegetation over the years. Similarly, for the end of the season (September), there is a slightly stronger positive trend
330 (r^2=0.13) with high interannual variation, indicating a later end of the season and a longer growing season.

https://doi.org/10.5194/egusphere-2024-3466
Preprint. Discussion started: 7 November 2024

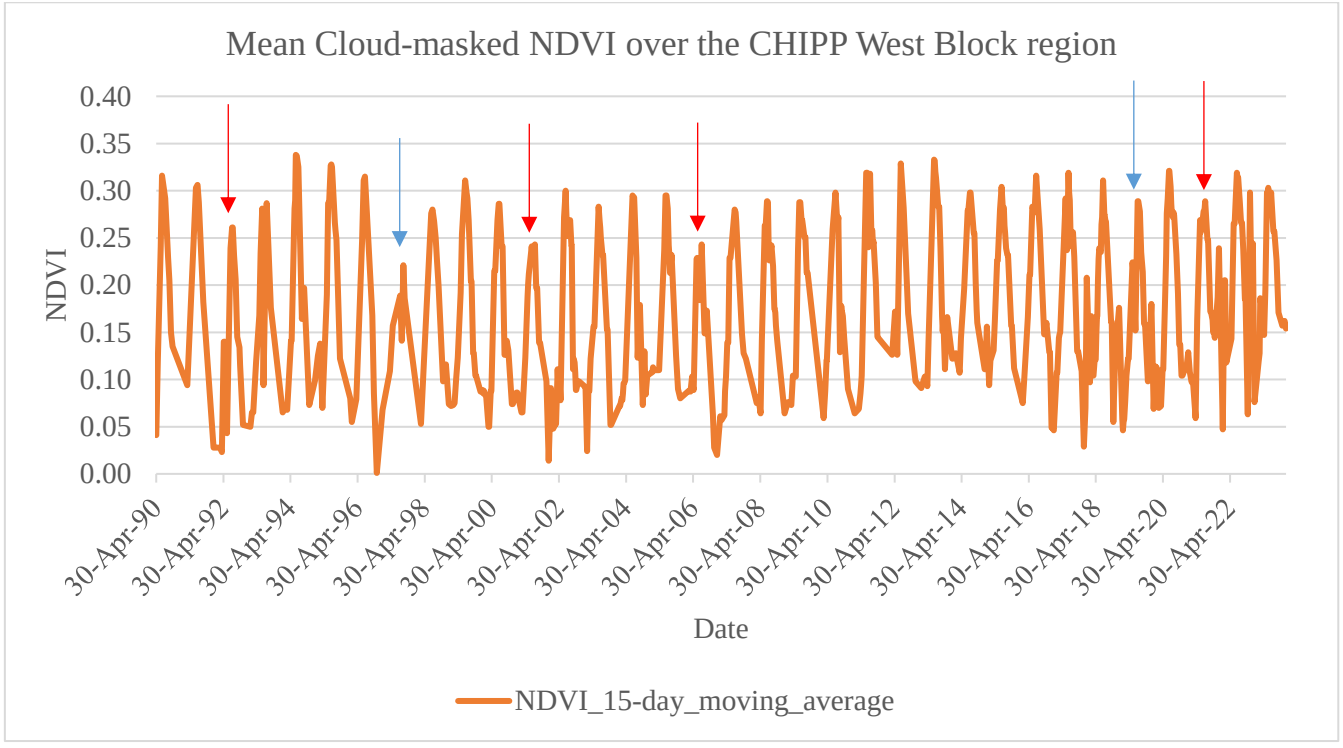

Figure 4 Smoothed out (15-day average) mean cloud masked NDVI time-series between 1990 and 2023 in the West Block of Cypress Hills Interprovincial Park, Saskatchewan, Canada

When comparing the mean annual NDVI trend with MAP and MAT, years with lower MAP and higher MAT, such as 2001, 2012, and 2021, correspond to lower mean annual NDVI values. Additionally, years with higher precipitation often result in increased NDVI in the following year (e.g., 1993, 1998, 2002, 2010, 2016, and 2019) (**Fig. 6**). This trend is more pronounced in the AHM index, where high AHM values during hot and dry years lead to lower NDVI values (**Fig. 7**).

https://doi.org/10.5194/egusphere-2024-3466
Preprint. Discussion started: 7 November 2024

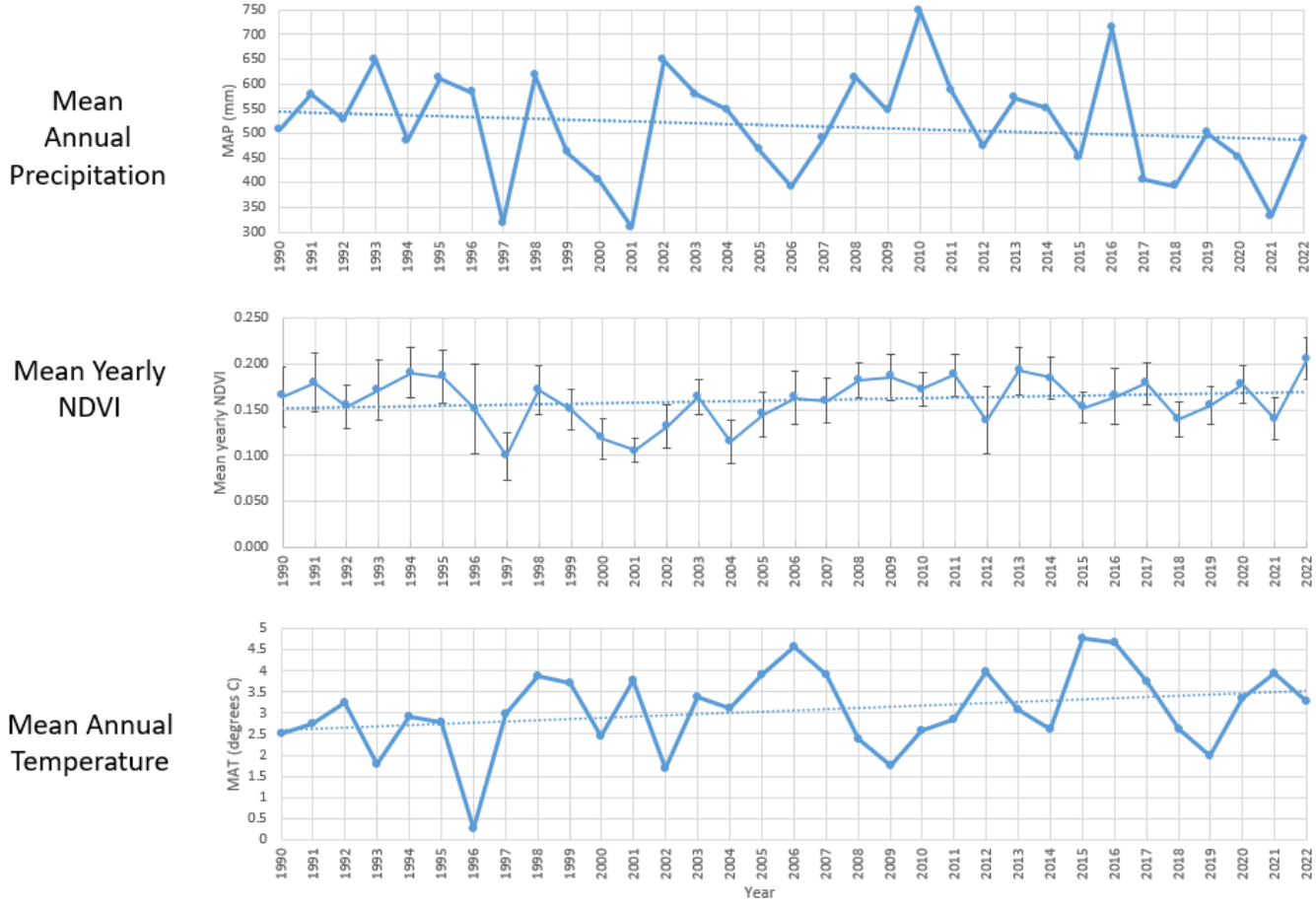

Figure 5 Mean annual NDVI versus mean annual precipitation (MAP) and mean annual temperature (MAT) between 1990 and 2023 in Cypress Hills Interprovincial Park, West Block (error bars depict the standard error).

https://doi.org/10.5194/egusphere-2024-3466
Preprint. Discussion started: 7 November 2024

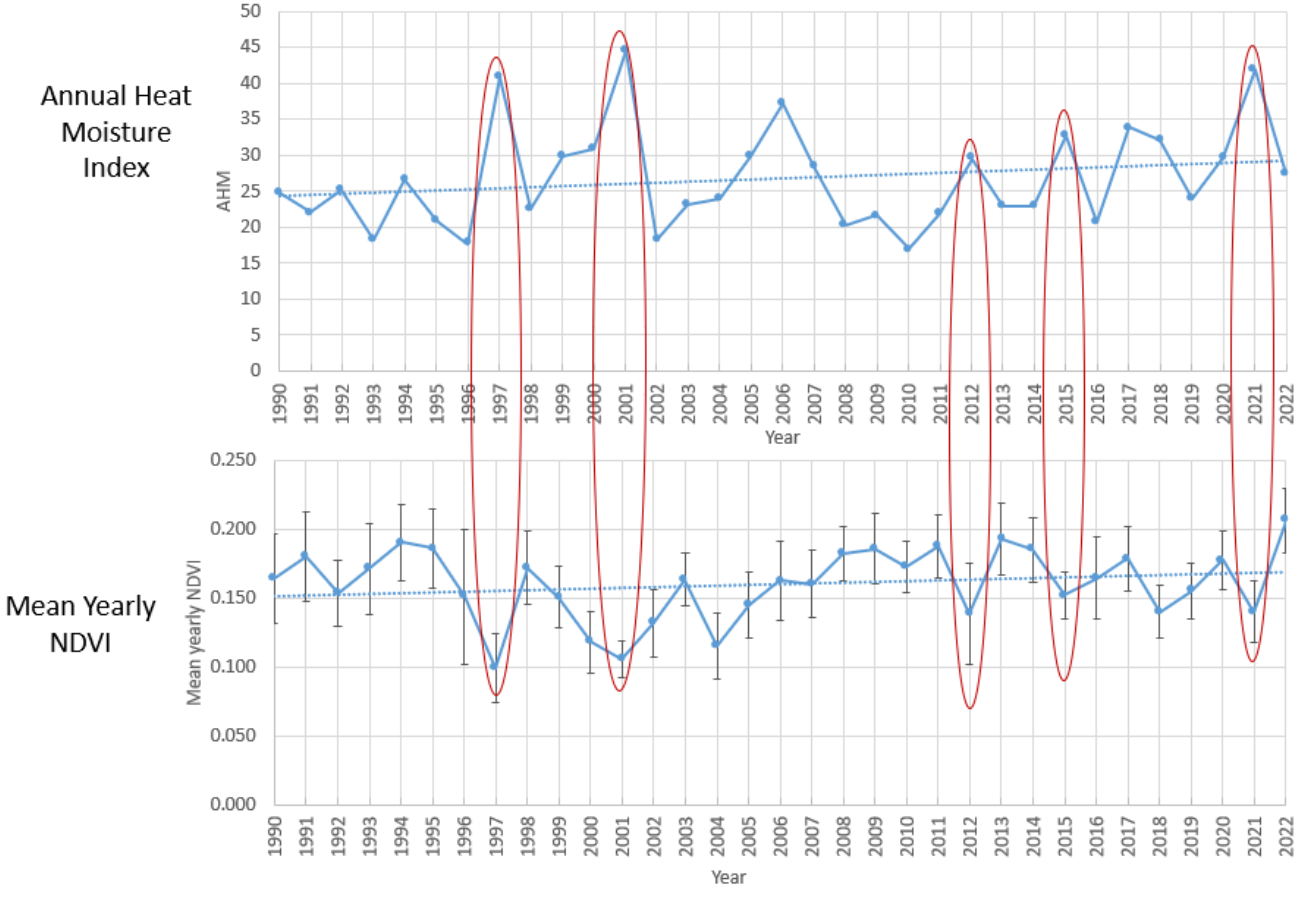

Figure 6 Mean annual NDVI versus the annual heat moisture index (AHM) between 1990 and 2023 in Cypress Hills Interprovincial Park, West Block (red circles indicate a combination of AHM peaks and NDVI lows, error bars depict the standard error).

345 ***Modeling***

The statistically significant results of each GLS model run are summarized in **Table 4**.

Topo-edaphic Models (Model 1a, b, c, d): 1a and 1b indicate that Loam Flat landscapes experienced a significant decrease in shrub cover change compared to Gravelly Flat landscapes. Additionally, 1c and 1d show that landscapes facing North, South, West, and East had a significant decrease in shrub cover change compared to Flat landscapes.

350 *Anthropogenic Models (Model 2):* Areas with low to medium grazing intensity saw an increase in shrub cover change between 2011 and 2018 compared to areas with high grazing intensity. Furthermore, areas hayed once between 2011 and 2018 exhibited a decrease in shrub cover change compared to areas that were not hayed at all.

Mixed Models (Model 3a1, a2, b1, b2): Shrub cover changes increased with rising slope percentages and proximity to roads. Additionally, 3a1 and 3b1 show that areas with low to medium grazing intensity experienced increases in shrub cover

https://doi.org/10.5194/egusphere-2024-3466
Preprint. Discussion started: 7 November 2024

compared to areas with high grazing intensity (similar to Model 2). There was also a decrease in shrub cover changes as the distance from watercourses and waterbodies in the park increased.

Table 4 GLS Model results (RSE=Residual Standard Error, AIC=Akaike Information Criterion, GLS=Generalized Least Squares (+) =statistically significant increase in shrub cover change (2011-2018), (-) =statistically significant decrease in shrub cover change (2011-2018)

Type	Model	Statistically important variables (*p*-value < 0.05)	RSE	AIC	Prediction error rate
Topo-edaphic	1a	Loam Flat (-) landscape unit compared to Gravelly Flat	3.94	98598.04	22.71
	1b		3.94	98595.90	22.71
	1c	1)[1] West (-) aspect compared to Flat, 2) South (-) aspect compared to Flat, 3) North (-) aspect compared to Flat, 4) East (-) aspect compared to Flat	4.05	15188.50	9.02
	1d		4.05	15183.50	9.02
Anthropogenic	2	1) Low-Medium grazing (+) compared to High grazing intensity, 2) Hayed one time (-) compared to no haying	4.10	40413.43	132.23
Mixed	3a1	1) Slope rise (+), 2) Low-Medium grazing (+) compared to High grazing intensity	3.91	39648.86	174.46
	3a2	Distance from watercourses (-)	4.30	4906.37	4.23
	3b1	1) Road distance (-), 2) Low-Medium grazing (+) compared to High grazing intensity, Medium-High grazing (+) compared to High grazing intensity	3.82	164699.6	22.66
	3b2	Distance from waterbodies (-)	3.91	55391.87	NA

[1]order of relative importance

3.3 Discussion

We found an annual percent shrub cover change in the grassland areas of the park close to 1% per year between 2011 and 2018. This estimate aligns with Barger et al. (2011) who reported that WPE increases by about 0.1-2.3% annually in North America. Higher estimates are observed in grasslands with greater rainfall, such as in Delgado's (2017) study, which found an annual increase of 1.96% in shrub cover in the tropical grasslands of Venezuela. Conversely, the annual percent shrub cover increase is lower in drier regions, as demonstrated by Marston & Aplin (2017), who found a 0.6% annual increase in the Southern African savanna.

https://doi.org/10.5194/egusphere-2024-3466
Preprint. Discussion started: 7 November 2024

Flat Loam ecosites show the highest shrub expansion, while Overflow ecosites maintain the most stable shrub cover due to their moisture-rich topographic position (Thorpe, 2007). Areas with a Very Fresh soil moisture regime and those near waterbodies also exhibit significant shrub expansion. This suggests that shrub expansion starts from stable patches in an appropriate micro-environment for establishment (S. R. Archer et al., 2017). Net shrub cover increases are observed in the park's wettest areas, and in the colder Uplands. The combined preference of shrubs for wetter and colder environments, as justified by the literature (Gxasheka et al., 2023), is evident in the AHM index patterns across the park. Higher shrub expansion as slope % rises can be supported by the notion that mean and steep slope levels have reduced cattle grazing (Bragg & Hulbert, 1976; Twidwell et al., 2013). Further, mid-slope soils could be closer to woody plant seeds, and woody plants can be more abundant on rock outcrops due to their protection from fire and grazing (Bragg & Hulbert, 1976).

From the anthropogenic factors, the road network contributes to shrub cover expansion, potentially facilitating shrub seed dispersal (Soubry et al., 2024). The highest shrub expansion rate was observed in Medium-High intensity grazed sites, while the lowest was in Low intensity grazed sites, likely due to cattle grazing patterns (Soubry et al., 2024). Haying practices also played a crucial role in reducing shrub cover changes, regardless of the year of haying. More recent and frequent haying practices within hayed areas significantly reduced shrub cover expansion.

Over the past 40 years, temperature, precipitation, and NDVI trends show significant interannual variation, primarily driven by drought and precipitation (Jiao et al., 2021). Our results indicate a later end of growing season, likely due to rising mean air temperatures (Linderholm, 2006). There is a clear link between precipitation and NDVI, a proxy for vegetation productivity, with a one-year lag observed between them. Indeed, vegetation productivity is limited by soil moisture, with a delayed response to precipitation noted in temperate forest-grassland ecotones (Liu et al., 2022). We found that low NDVI values often coincide with temperature peaks, similar to Yang et al. (2023), reflecting vegetation's vulnerability to drought. However, these NDVI patterns may be more influenced by grasses than shrubs (Browning et al., 2017).

3.3.1 Limitations

We used a post-classification change detection method, which propagates the errors of each image classification into the final change detection layer. A change classification approach, where all bands are stacked into a single image and then classified, could be more effective. Additionally, there were limitations in the aerial images. The years and seasons of the image acquisitions did not match the field data collections, potentially leading to misclassifications from seasonal differences. Moreover, the driving factor analysis did not include the "No shrub cover" class. Future work could incorporate this class to better understand areas not preferred by shrubs. Lastly, without long-term fire history for the park due to fire suppression we could not investigate fire impact on shrub cover.

https://doi.org/10.5194/egusphere-2024-3466
Preprint. Discussion started: 7 November 2024

Acknowledgements

The authors acknowledge the FlySask program for providing aerial imagery. We also thank Larissa Robinov, Lampros Nikolaos Maros, Kyle Cuthbert, Chiara Richiardi, Dr. Fei Xing, Dr. Yanmei Mu, Olokeogun Oluwayemisi, and Dr. Xiaolei Yu for their fieldwork assistance in the West Block of CHIPP.

References

Archer, S., Boutton, T. W., & Hibbard, K. A. (2001). Trees in Grasslands: Biogeochemical Consequences Woody Plant Expansion. In *Global Biogeochemical Cycles in the Climate System* (pp. 115–137). Academic Press.

Archer, S. R., Andersen, E. M., Predick, K. I., Schwinning, S., Steidl, R. J., & Woods, S. R. (2017). Woody Plant Encroachment-Causes and Concequences. In D. D. Briske (Ed.), *Rangeland Systems-Processes, Management and Challenges* (pp. 25–84). Springer Series on Environmental Management, Springer. https://doi.org/10.1007/978-3-319-46709-2_2

Bailey, A. W., McCartney, D., & Schellenberg, M. P. (2010). *Management of Canadian Prairie Rangeland* (AAFC No. 10144).

Bardgett, R. D., Bullock, J. M., Lavorel, S., Manning, P., Schaffner, U., Ostle, N., Chomel, M., Durigan, G., L. Fry, E., Johnson, D., Lavallee, J. M., Le Provost, G., Luo, S., Png, K., Sankaran, M., Hou, X., Zhou, H., Ma, L., Ren, W., … Shi, H. (2021). Combatting global grassland degradation. *Nature Reviews Earth & Environment*, *2*(10), 720–735. https://doi.org/10.1038/s43017-021-00207-2

Barger, N. N., Archer, S. R., Campbell, J. L., Huang, C. Y., Morton, J. A., & Knapp, A. K. (2011). Woody plant proliferation in North American drylands: A synthesis of impacts on ecosystem carbon balance. *Journal of Geophysical Research: Biogeosciences*, *116*(3), 1–17. https://doi.org/10.1029/2010JG001506

Beck, J. J., Hernández, D. L., Pasari, J. R., & Zavaleta, E. S. (2015). Grazing maintains native plant diversity and promotes community stability in an annual grassland. *Ecological Applications*, *25*(5), 1259–1270. https://doi.org/10.1890/14-1093.1

Bogunovic, I., Fernandez, M. P., Kisic, I., & Marimon, M. B. (2019). Agriculture and grazing environments. *Advances in Chemical Pollution, Evironmental Management and Protection*, *4*, 23–70. https://doi.org/10.1016/bs.apmp.2019.07.005

Bond, W. J., & Midgley, G. F. (2000). A proposed CO2-controlled mechanism of woody plant invasion in grasslands and savannas. *Global Change Biology*, *6*(8), 865–869. https://doi.org/10.1046/j.1365-2486.2000.00365.x

Bond, W. J., & Midgley, G. F. (2012). Carbon dioxide and the uneasy interactions of trees and savannah grasses. *Philosophical Transactions of the Royal Society B: Biological Sciences*, *367*(1588), 601–612. https://doi.org/10.1098/rstb.2011.0182

Bragg, T. B., & Hulbert, L. C. (1976). Woody Plant Invasion of Unburned Kansas Bluestem Prairie. *Journal of Range Management*, *29*(1), 19–24.

https://doi.org/10.5194/egusphere-2024-3466
Preprint. Discussion started: 7 November 2024

http://www.jstor.org/stable/3897682%5Cnhttp://www.jstor.org/%5Cnhttp://www.jstor.org/action/showPublisher?publisherCode=acg.

Briggs, J. M., Knapp, A. K., Blair, J. M., Heisler, J. L., Hoch, G. A., Lett, M. S., & McCarron, J. K. (2005). An ecosystem in transition: Causes and consequences of the conversion of mesic grassland to shrubland. *BioScience*, *55*(3), 243–254. https://doi.org/10.1641/0006-3568(2005)055[0243:AEITCA]2.0.CO;2

Briske editor, D. D. (2017). *Rangeland Systems-Processes, Management and Challenges* (D. D. Briske (ed.)). SpringerOpen. https://doi.org/10.1007/978-3-319-46709-2_2

Browning, D. M., Franklin, J., Archer, S. R., Gillan, J. K., Guertin, D. P., Browning, D. M., Franklin, J., Archer, S. R., Gillan, J. K., & Guertin, D. P. (2014). Spatial patterns of grassland — shrubland state transitions: a 74-year record on grazed and protected areas. *Ecological Applications*, *24*(6), 1421–1433.

Browning, D. M., Karl, J. W., Morin, D., Richardson, A. D., & Tweedie, C. E. (2017). Phenocams bridge the gap between field and satellite observations in an arid grassland ecosystem. *Remote Sensing*, *9*(10). https://doi.org/10.3390/rs9101071

Buenemann, M. (2007). *Quantifying the spatio-temporal dynamics of woody plant encroachment using an integrative remote sensing, GIS, and spatial modelling approach*. University of Oklahoma.

Cheng, W., Dan, L., Deng, X., Feng, J., Wang, Y., Peng, J., Tian, J., Qi, W., Liu, Z., Zheng, X., Zhou, D., Jiang, S., Zhao, H., & Wang, X. (2022). Global monthly gridded atmospheric carbon dioxide concentrations under the historical and future scenarios. *Scientific Data*, *9*(1), 1–13. https://doi.org/10.1038/s41597-022-01196-7

Delgado, A. S. (2017). *Assessment of long-term effects of woody plant expansion in a humid, tropical grassland of Venezuela*. University of Texas Rio Grande Valley.

Eldridge, D. J., Soliveres, S., Bowker, M. A., & Val, J. (2013). Grazing dampens the positive effects of shrub encroachment on ecosystem functions in a semi-arid woodland. *Journal of Applied Ecology*, *50*(4), 1028–1038. https://doi.org/10.1111/1365-2664.12105

FAO. (1995). *Forest Resources Assessment 1990 - Global Synthesis - FAO Forestry Paper 124*. https://www.fao.org/3/v5695e/v5695e00.htm

Gartzia, M., Alados, C. L., & Pérez-Cabello, F. (2014). Assessment of the effects of biophysical and anthropogenic factors on woody plant encroachment in dense and sparse mountain grasslands based on remote sensing data. *Progress in Physical Geography*, *38*(2), 201–217. https://doi.org/10.1177/0309133314524429

Gavier-Pizarro, G. I., Kuemmerle, T., Hoyos, L. E., Stewart, S. I., Huebner, C. D., Keuler, N. S., & Radeloff, V. C. (2012). Monitoring the invasion of an exotic tree (Ligustrum lucidum) from 1983 to 2006 with Landsat TM/ETM+ satellite data and Support Vector Machines in Córdoba, Argentina. *Remote Sensing of Environment*, *122*, 134–145. https://doi.org/10.1016/j.rse.2011.09.023

Ghulam, A., Freeman, K., Bollen, A., Ripperdan, R., & Porton, I. (2011). Mapping invasive plant species in tropical rainforest using polarimetric Radarsat-2 and PALSAR data. *International Geoscience and Remote Sensing Symposium (IGARSS)*, 3514–3517. https://doi.org/10.1109/IGARSS.2011.6049979

https://doi.org/10.5194/egusphere-2024-3466
Preprint. Discussion started: 7 November 2024

Gray, E. F., & Bond, W. J. (2013). Will woody plant encroachment impact the visitor experience and economy of conservation areas? *Koedoe*, *55*(1), 1–9. https://doi.org/10.4102/koedoe.v55i1.1106

Gxasheka, M., Sabelo, C., & Dlamini, P. (2023). The role of topographic and soil factors on woody plant encroachment in mountainous rangelands : A mini literature review. *Heliyon*, *9*(10), e20615. https://doi.org/10.1016/j.heliyon.2023.e20615

He, K. S., Rocchini, D., Neteler, M., & Nagendra, H. (2011). Benefits of hyperspectral remote sensing for tracking plant invasions. *Diversity and Distributions*, *17*(3), 381–392. https://doi.org/10.1111/j.1472-4642.2011.00761.x

Hendrickson, J. R., Sedivec, K. K., Toledo, D., & Printz, J. (2019). Challenges Facing Grasslands inthe Northern Great Plains and North Central Region. *Rangelands*, *41*(1), 23–29. https://doi.org/10.1016/j.rala.2018.11.002

Hewins, D. B., Lyseng, M. P., Schoderbek, D. F., Alexander, M., Willms, W. D., Carlyle, C. N., Chang, S. X., & Bork, E. W. (2018). Grazing and climate effects on soil organic carbon concentration and particle-size association in northern grasslands. *Scientific Reports*, *8*(1), 1–9. https://doi.org/10.1038/s41598-018-19785-1

Jensen, J. R. (2008). *Remote sensing of the environment: An Earth Resource Perspective* (2nd ed.). Pearson Education, Inc.

Jiao, K., Gao, J., & Liu, Z. (2021). Precipitation drives the ndvi distribution on the tibetan plateau while high warming rates may intensify its ecological droughts. *Remote Sensing*, *13*(7). https://doi.org/10.3390/rs13071305

Jose Pinheiro, Bates, D., DebRoy, S., Sarkar, D., & R Development Core Team. (2013). *nlme: Linear and Nonlinear Mixed Effects Models. R package* (3.1-108). R Core Team.

Kennedy, B. A. (1976). Valley-side Slopes and Climate. *Geomorphology and Climate*, 185–187.

Kopeć, D., Zakrzewska, A., Halladin-Dąbrowska, A., Wylazłowska, J., Kania, A., & Niedzielko, J. (2019). Using Airborne Hyperspectral Imaging Spectroscopy to Accurately Monitor Invasive and Expansive Herb Plants: Limitations and Requirements of the Method. *Sensors*, *19*(13), 2871. https://doi.org/10.3390/s19132871

Körner, C. (2006). Plant CO2 responses: An issue of definition, time and resource supply. *New Phytologist*, *172*(3), 393–411. https://doi.org/10.1111/j.1469-8137.2006.01886.x

Kwon, H.-Y., Nkonya, E., Johnson, T., Graw, V., Kato, E., & Kihiu, E. (2016). Global estimates of the impacts of grassland degradation on livestock productivity from 2001 to 2011. In E. Nkonya, A. Mirzabaev, & J. von Braun (Eds.), *Economics of Land Degradation and Improvement - A Global Assessment for Sustainable Development* (pp. 197–214). Springer. https://doi.org/10.1007/978-3-319-19168-3

Lane, D. M. (2008). Graphing Distributions, section "Histograms." In *Online Statistics Education: A Multimedia Course of Study* (2nd ed.). Rice University (Lead Developer), University of Houston Clear Lake, and Tufts University. http://onlinestatbook.com/

Lass, L. W., Prather, T. S., Glenn, N. F., Weber, K. T., Mundt, J. T., & Pettingill, J. (2005). A review of remote sensing of invasive weeds and example of the early detection of spotted knapweed (Centaurea maculosa) and babysbreath (Gypsophila paniculata) with a hyperspectral sensor. *Weed Science*, *53*(2), 242–251. https://doi.org/10.1614/ws-04-044r2

Linderholm, H. W. (2006). Growing season changes in the last century. *Agricultural and Forest Meteorology*, *137*(1–2), 1–14. https://doi.org/10.1016/j.agrformet.2006.03.006

https://doi.org/10.5194/egusphere-2024-3466
Preprint. Discussion started: 7 November 2024

Liu, X., Tian, Y., Liu, S., Jiang, L., Mao, J., Jia, X., Zha, T., Zhang, K., Wu, Y., & Zhou, J. (2022). Time-Lag Effect of Climate Conditions on Vegetation Productivity in a Temperate Forest–Grassland Ecotone. *Forests*, *13*(7), 1–20. https://doi.org/10.3390/f13071024

Ma, S., Zhou, Y., Gowda, P. H., Chen, L., Starks, P. J., Steiner, J. L., & Neel, J. P. S. (2019). Evaluating the impacts of continuous and rotational grazing on tallgrass prairie landscape using high-spatial-resolution imagery. *Agronomy*, *9*(5). https://doi.org/10.3390/agronomy9050238

Marston, C. G., Aplin, P., Wilkinson, D. M., Field, R., & O'Regan, H. J. (2017). Scrubbing up: Multi-scale investigation of woody encroachment in a Southern African savannah. *Remote Sensing*, *9*(5). https://doi.org/10.3390/rs9050419

Mazía, N., Chaneton, E. J., & Ghersa, C. M. (2019). Disturbance types, herbaceous composition, and rainfall season determine exotic tree invasion in novel grassland. *Biological Invasions*, *21*(4), 1351–1363. https://doi.org/10.1007/s10530-018-1906-x

Millan, V. G., & Sanchez-Azofeifa, A. (2018). Quantifying changes on forest succession in a dry tropical forest using angular-hyperspectral remote sensing. *Remote Sensing*, *10*(12). https://doi.org/10.3390/rs10121865

Morford, S. L., Allred, B. W., Twidwell, D., Jones, M. O., Maestas, J. D., Roberts, C. P., & Naugle, D. E. (2022). Herbaceous production lost to tree encroachment in United States rangelands. *Journal of Applied Ecology*, *59*(12), 2971–2982. https://doi.org/10.1111/1365-2664.14288

Moss, R., Gardiner, B., Bailey, A., & Oliver, G. (2008). *A guide to integrated Brush Management on the Western Canadian Plains*.

O'Connor, C. R. (2019). *Drivers, mechanisms, and thresholds of woody encroachment in mesic grasslands*. Kansas State University.

Oldeland, J., Dorigo, W., Wesuls, D., & Jürgens, N. (2010). Mapping bush encroaching species by seasonal differences in hyperspectral imagery. *Remote Sensing*, *2*(6), 1416–1438. https://doi.org/10.3390/rs2061416

Parelius, E. J. (2023). A Review of Deep-Learning Methods for Change Detection in Multispectral Remote Sensing Images. *Remote Sensing*, *15*(8). https://doi.org/10.3390/rs15082092

Polley, H. W., Briske, D. D., Morgan, J. A., Wolter, K., Derek, W., Polley, H. W., Briske, D. D., Morgan, J. A., Wolter, K., Bailey, D. W., & Brown, J. R. (2013). Climate Change and North American Rangelands: Trends , Projections , and Implications. *Rangeland Ecology and Management*, *66*(5), 493–511.

Pracilio, G., Smettem, K. R. J., Bennett, D., Harper, R. J., & Adams, M. L. (2006). Site assessment of a woody crop where a shallow hardpan soil layer constrained plant growth. *Plant and Soil*, *288*(1–2), 113–125. https://doi.org/10.1007/s11104-006-9098-z

Puyravaud, J. P. (2003). Standardizing the calculation of the annual rate of deforestation. *Forest Ecology and Management*, *177*(1–3), 593–596. https://doi.org/10.1016/S0378-1127(02)00335-3

https://doi.org/10.5194/egusphere-2024-3466
Preprint. Discussion started: 7 November 2024

Rajah, P., Odindi, J., Mutanga, O., & Kiala, Z. (2019). The utility of Sentinel-2 Vegetation Indices (VIs) and Sentinel-1 Synthetic Aperture Radar (SAR) for invasive alien species detection and mapping. *Nature Conservation*, *35*, 41–61. https://doi.org/10.3897/natureconservation.35.29588

Royimani, L., Mutanga, O., Odindi, J., Dube, T., & Matongera, T. N. (2019). Advancements in satellite remote sensing for mapping and monitoring of alien invasive plant species (AIPs). *Physics and Chemistry of the Earth, Parts A/B/C*, *112*, 237–245. https://doi.org/10.1016/j.pce.2018.12.004

RStudio Team. (2021). *RStudio: Integrated Development Environment for R* (2021.9.1.372). RStudio, PBC. http://www.rstudio.com/

Scholtz, R., Fuhlendorf, S. D., & Archer, S. R. (2018). Climate–fire interactions constrain potential woody plant cover and stature in North American Great Plains grasslands. *Global Ecology and Biogeography*, *27*(8), 936–945. https://doi.org/10.1111/geb.12752

Scholtz, R., Polo, J. A., Fuhlendorf, S. D., Engle, D. M., & Weir, J. R. (2018). Woody Plant Encroachment Mitigated Differentially by Fire and Herbicide. *Rangeland Ecology and Management*, *71*(2), 239–244. https://doi.org/10.1016/j.rama.2017.10.001

Skowno, A. L., Thompson, M. W., Hiestermann, J., Ripley, B., West, A. G., & Bond, W. J. (2017). Woodland expansion in South African grassy biomes based on satellite observations (1990–2013): general patterns and potential drivers. *Global Change Biology*, *23*(6), 2358–2369. https://doi.org/10.1111/gcb.13529

Skowronek, S., Ewald, M., Isermann, M., Van De Kerchove, R., Lenoir, J., Aerts, R., Warrie, J., Hattab, T., Honnay, O., Schmidtlein, S., Rocchini, D., Somers, B., & Feilhauer, H. (2017). Mapping an invasive bryophyte species using hyperspectral remote sensing data. *Biological Invasions*, *19*(1), 239–254. https://doi.org/10.1007/s10530-016-1276-1

Smith, A. M., & Buckley, J. R. (2011). Investigating RADARSAT-2 as a tool for monitoring grassland in western Canada. *Canadian Journal of Remote Sensing*, *37*(1), 93–102. https://doi.org/10.5589/m11-027

Soubry, I., & Guo, X. (2021). Identification of the Optimal Season and Spectral Regions for Shrub Cover Estimation in Grasslands. *Sensors*, *21*(3098), 1–26. https://doi.org/https://doi.org/ 10.3390/s21093098

Soubry, I., & Guo, X. (2022). Quantifying Woody Plant Encroachment in Grasslands: A Review on Remote Sensing Approaches. *Canadian Journal of Remote Sensing*, 1–42. https://doi.org/10.1080/07038992.2022.2039060

Soubry, I., Robinov, L., Chu, T., & Guo, X. (2024). Identifying anthropogenic and fixed influencing factors of shrub encroachment in Cypress Upland, Canada - Under Review. *Heliyon*.

Soubry, I., Robinov, L., Chu, T., & Xulin, G. (2022). Mapping shrub cover in grasslands with an object-based approach and investigating the connection to topo-edaphic factors. *Geocarto International*, 1–16.

Statistics Canada. (2020). *2016 Census-Boundary files*. https://www12.statcan.gc.ca/census-recensement/2011/geo/bound-limit/bound-limit-2016-eng.cfm

Stevens, N., Lehmann, C. E. R., Murphy, B. P., & Durigan, G. (2017). Savanna woody encroachment is widespread across three continents. *Global Change Biology*, *23*(1), 235–244. https://doi.org/10.1111/gcb.13409

https://doi.org/10.5194/egusphere-2024-3466
Preprint. Discussion started: 7 November 2024

Strassburg, B. B. N., Iribarrem, A., & Beyer, H. L. (2020). *Global priority areas for ecosystem restoration*. *August 2019*. https://doi.org/10.1038/s41586-020-2784-9

Sturges, H. A. (1926). The Choice of a Class Interval. *Journal of the American Statistical Association*, *21*(153), 65–66. https://doi.org/10.1080/01621459.1926.10502161

Thornton, M. M. R., Shrestha, Y. W., Thornton, P. E., Kao, S.-C., & Wilson, B. E. (2022). *Daymet: Daily Surface Weather Data on a 1-km Gird for North America, Version 4 R1*. ORNL DAAC, Oak Ridge, Tennessee, USA. https://doi.org/https://doi.org/10.3334/ORNLDAAC/2129

Thorpe, J. (2007). Saskatchewan Rangeland Ecosystems, Publication 1: Ecoregions and Ecosites. In *Saskatchewan Prairie Conservation Action Plan*. Alberta: Saskatchewan Research Council.

Twidwell, D., Rogers, W. E., Fuhlendorf, S. D., Wonkka, C. L., Engle, D. M., Weir, J. R., Kreuter, U. P., & Taylor, C. A. (2013). The rising Great Plains fire campaign: Citizens' response to woody plant encroachment. *Frontiers in Ecology and the Environment*, *11*(1), e64–e71. https://doi.org/10.1890/130015

Van Auken, O. W. (2000). Shrub Invasions of North American Semiarid Grasslands. *Annual Review of Ecology and Systematics*, *31*(2000), 197–215.

Venter, Z. S., Cramer, M. D., & Hawkins, H. J. (2018). Drivers of woody plant encroachment over Africa. *Nature Communications*, *9*(1), 1–7. https://doi.org/10.1038/s41467-018-04616-8

Wang, G., Li, J., & Ravi, S. (2019). A combined grazing and fire management may reverse woody shrub encroachment in desert grasslands. *Landscape Ecology*, *34*(8), 2017–2031. https://doi.org/10.1007/s10980-019-00873-0

Wilsey, B. J. (2018). *The Biology of Grasslands* (First). Oxford University Press. https://doi.org/10.1093/oso/9780198744511.001.0001

Yang, Q., Jiang, C., & Ding, T. (2023). Impacts of Extreme-High-Temperature Events on Vegetation in North China. *Remote Sensing*, *15*(18). https://doi.org/10.3390/rs15184542

Zlinszky, A., Schroiff, A., Kania, A., Deák, B., Mücke, W., Vári, Á., Székely, B., & Pfeifer, N. (2014). Categorizing grassland vegetation with full-waveform airborne laser scanning: A feasibility study for detecting natura 2000 habitat types. *Remote Sensing*, *6*(9), 8056–8087. https://doi.org/10.3390/rs6098056